

# Hubble selection of the weak scale from QCD quantum critical point

Sunghoon Jung<sup>1,2,\*</sup> and TaeHun Kim<sup>1,†</sup>

<sup>1</sup>*Center for Theoretical Physics, Department of Physics and Astronomy, Seoul National University, Seoul 08826, Korea*

<sup>2</sup>*Astronomy Research Center, Seoul National University, Seoul 08826, Korea*

There is growing evidence that the small weak scale may be related to self-organized criticality. In this regard, we note that if the strange quark were lighter, the QCD phase transition could have been first order, possibly exhibiting quantum critical points at zero temperature as a function of the Higgs vacuum expectation value  $v_h$  smaller than (but near) the weak scale. We show that these quantum critical points allow a dynamical selection of the observed weak scale, via quantum-dominated stochastic evolutions of the value of  $v_h$  during eternal inflation. Although the values of  $v_h$  in different Hubble patches are described by a probability distribution in the multiverse, inflationary quantum dynamics ensures that the peak of the distribution evolves toward critical points (self-organized criticality), driven mainly by the largest Hubble expansion rate there – the Hubble selection of the universe. To this end, we first explore the quantum critical points of the three-flavor QCD linear sigma model, parametrized by  $v_h$  at zero temperature, and we present a relaxation model for the weak scale. Among the patches that have reached reheating, it results in a sharp probability distribution of  $v_h$  near the observed weak scale, which is critical not to the crossover at  $v_h = 0$  but to the sharp transition at  $\sim \Lambda_{\text{QCD}}$ .

## I. INTRODUCTION

The Planck weak-scale hierarchy may be addressed by the near criticality of the Higgs mass parameter [1, 2]. In this viewpoint, the small weak scale close to zero is special because the universe transitions between broken and unbroken phases of the electroweak symmetry at zero. The transition could generate various standard model (SM) backreactions that allow dynamical selection of the weak scale [3–8]. However, this transition is a second-order crossover in the SM, providing only relatively smooth selection rules. In addition, the SM Higgs potential, once renormalization-group evolved, was found to yield another almost degenerate vacuum near the Planck scale [9, 10]. This surprising coincidence provides more evidence that the particular (seemingly unnatural) value of the weak scale might be related to criticality. This motivated ideas of multiple-point principle [11–15], classical scale invariance [16–18], as well as Higgs inflation [19–21]. Extremely small dark energy is also thought to be near the critical point. But yet, whether and how criticality plays a crucial role in naturalness remain unclear.

Recently, a cosmological selection mechanism for criticality was developed in Ref. [22], where inflationary quantum-dominated evolution of the relaxation inevitably drives a theory parameter close to a quantum critical point. In one setup, it is crucial that the critical point be the first-order separation between discrete phases with a significant energy difference, so that the Hubble rate can be sharply largest there. Then after long enough inflation (essentially eternal as will be discussed), such Hubble patches having a theory near the critical point

will dominate the multiverse, as they are expanding and are reproduced most rapidly – Hubble selection of the universe. This mechanism realizes self-organized criticality [22]; see also Refs. [23, 24].

Then we ask the following: Why is the selection of criticality the selection of the observed small weak scale? To what first-order critical points does the Higgs mass have relevance? Reference [22] analyzed the aforementioned renormalization-scale dependence of the SM Higgs vacuum structure [9, 10], but the critical scale was found to be far above the weak scale. References [5, 6] studied a prototype model with multiple axions, where a QCD barrier trapping an axion disappears when  $v_h$  turns off, so that the axion suddenly rolls down to the minimum, generating a large energy contrast necessary for Hubble selection. Critical changes of a theory could also induce the small weak scale in association with much smaller dark energy [7, 8].

In this Letter, we present a cosmological account of the weak scale from possible first-order zero-temperature (hence, quantum) critical points of QCD.<sup>1</sup> We first point out that QCD may have built-in quantum critical points at some  $v_h^* \lesssim v_{\text{EW}} = 246 \text{ GeV}$ ; this has yet to be studied, and we initiate an exploration using the three-flavor linear sigma model (LSM) of low-energy QCD. Then we present a relaxation model that realizes Hubble selection of the QCD criticality and self-organizes  $v_h$  close to the observed value. Then,  $v_h$  is critical to  $\sim \Lambda_{\text{QCD}}$  (not to the crossover at zero). An added benefit is that the weak scale and  $\Lambda_{\text{QCD}}$  are generically close, which otherwise is accidental. Furthermore, building upon earlier works, we elaborate Hubble selection with different semi quantitative derivations.

\* sunghoonj@snu.ac.kr

† gimthcha@snu.ac.kr

<sup>1</sup> The small weak scale, if not due to criticalities or symmetries, could also be a result of the cosmological selection of anthropic [7, 25–29] or entropic [30–35] principles in a multiverse.

We are inspired by observations that if the strange quark were slightly lighter, the (finite-temperature  $T$ ) QCD chiral phase transition could have been first order. Although not yet firmly established [36–43], this possibility has been expected based on the (non)existence of infrared fixed points in the three-dimensional LSM [44, 45]. In other words, QCD at  $T = 0$  too (relevant during inflation) may have a rich vacuum structure, as a function of variable quark masses or  $v_h$ . Our initial phenomenological exploration of the vacuum structure shall be verified by dedicated research.

The Letter discusses the basic model ingredients (Sec. II), exploration of QCD quantum critical points (Sec. III), Hubble selection (Sec. IV), realization of the weak-scale criticality (Sec. V), and conclusions with future improvements.

## II. MODEL

The model consists of the relaxion  $\phi$  [3], the Higgs  $h$ , and the meson field  $\Sigma$ :  $V_{\text{tot}} = V_\phi + V_h + V_\Sigma$ . The relaxion couples only to the Higgs sector, scanning  $v_h$ . But the change of  $v_h$  induces changes in the  $\Sigma$  sector, developing the desired quantum criticality at  $v_h^*$ . Then the Hubble selection (acting on  $\phi$ ) self-organizes the universe to the critical point.

The real-scalar relaxion potential is axion like:

$$V_\phi = \Lambda_\phi^4 \cos \frac{\phi}{f_\phi}. \quad (1)$$

For Hubble selection, its field range  $f_\phi$  shall exceed the Planck scale (see later), which is possible with multiple axions [46–48].

The Higgs potential takes the SM form ( $\lambda_h \simeq 0.13$ ) plus the coupling to the relaxion (see Ref. [3] for details)

$$V_h = \frac{1}{2}(M^2 - g\tilde{\phi})h^2 + \frac{\lambda_h}{4}h^4 \rightarrow -\frac{1}{2}(g\phi)h^2 + \frac{\lambda_h}{4}h^4, \quad (2)$$

where  $h$  is the real Higgs field in unitary gauge. We shift  $\phi$  such that the quadratic term  $\mu_h^2 = -g\phi$  vanishes at  $\phi=0$ .  $v_h^2 \equiv -\mu_h^2/\lambda_h = g\phi/\lambda_h$  is used to label the relaxion scanning ( $v_{\text{EW}} = 246$  GeV).<sup>2</sup> The required field range of  $\phi$  to scan  $\mu_h^2$  up to the cutoff  $M^2$  is  $\delta\phi \sim M^2/g$ , thus we set  $f_\phi = M^2/g$ . The dimensionful coupling  $g$  is a spurion of the relaxion shift symmetry, and thus can be small naturally.

Below  $\Lambda_{\text{QCD}} = 200$  MeV, meson fields  $\Sigma_{ij}(x)$  are relevant degrees of freedom, whose condensates are order parameters for chiral symmetry breaking. This vacuum

structure as a function of  $v_h$  is what we want to explore. It can be conveniently described by the LSM with  $U(N_f)_L \times U(N_f)_R$  symmetry of QCD [49–51],

$$V_\Sigma = \mu^2 \text{Tr}[\Sigma \Sigma^\dagger] + \lambda_1 (\text{Tr}[\Sigma \Sigma^\dagger])^2 + \lambda_2 \text{Tr}[(\Sigma \Sigma^\dagger)^2] - c(\det \Sigma + \det \Sigma^\dagger) - \text{Tr}[\mathcal{H}(\Sigma + \Sigma^\dagger)], \quad (3)$$

where fields and parameters are decomposed as  $\Sigma = (\sigma_a + i\pi_a)T^a$ ,  $\mathcal{H} = h_a T^a$  with generators  $T^a$  satisfying  $\text{Tr}[T^a T^b] = \delta^{ab}/2$  for  $a = 0, \dots, N_f^2 - 1$ . Without losing generality,  $\lambda_{1,2}, h_a$  are real,  $c > 0$ , and  $\mu^2$  can take either sign.  $\Sigma$  is bifundamental under the symmetry. The first line of Eq. (3) conserves  $SU(N_f)_L \times SU(N_f)_R$ ;  $\lambda_2$  is nonzero, otherwise symmetry is enhanced to  $O(2N_f^2)$ . One of the remaining  $U(1)$ 's is identified as the conserved baryon number  $U(1)_V$ , simply omitted in our discussion. The other  $U(1)_A$  is anomalous, broken by the instanton contribution  $c$  down to  $Z_A(N_f)$  [52, 53]. Symmetries are further broken by  $\mathcal{H}$ , the leading chiral-symmetry-breaking mass term. We fix  $N_f = 3$  with the isospin symmetry  $m_u = m_d$ , as a first exploration; only  $h_0, h_8 \neq 0$ .

It is worthwhile to note that the LSM indeed possesses necessary features for quantum critical points. For  $N_f = 3$ , the instanton term is a cubic potential, possibly creating local vacua (even with  $\mu^2 > 0$ ). The linear term  $\mathcal{H}$  can destabilize the local vacua at critical quark masses or  $v_h^*$ , just as the external magnetic field (the linear term) in ferromagnets flips higher-energy spin directions at a critical field strength.

## III. QCD QUANTUM CRITICAL POINTS

To explore the vacuum structure as a function of  $v_h$ , we first fix the benchmark ‘‘SM point’’ parameters of  $V_\Sigma$ , reproducing a measured meson spectrum, and then we deduce how these parameters change with  $v_h$ .

The masses of pions and kaons, being pseudo-Goldstones, are given by symmetry-breaking terms  $\mathcal{H}$ , related by partially conserved axial-vector currents,

$$\partial_\mu j_a^{\mu 5} = m_{\pi_a}^2 f_{\pi_a} \pi_a = \pi_b h_c d_{abc}, \quad (4)$$

where the last equality is obtained by the variation of  $V_\Sigma$  under chiral transformations. For pions  $\pi^0 = \pi_3$  with  $d_{3b0} = \sqrt{2/3}\delta_{b3}, d_{3b8} = 1/\sqrt{3}\delta_{b3}$ , and for kaons  $K^0 = (\pi_6 + i\pi_7)/\sqrt{2}$  with  $d_{Kb0} = \sqrt{2/3}\delta_{bK}, d_{Kb8} = -1/\sqrt{12}\delta_{bK}$ , we have

$$m_\pi^2 f_\pi = \sqrt{\frac{2}{3}}h_0 + \frac{h_8}{\sqrt{3}}, \quad m_K^2 f_K = \sqrt{\frac{2}{3}}h_0 - \frac{h_8}{2\sqrt{3}}. \quad (5)$$

Using measured values of  $m_{\pi,K}$  (Table I), we fix the SM-point value of  $h_{0,8}$  [54],

$$h_0(v_{\text{EW}}) = (287 \text{ MeV})^3, \quad h_8(v_{\text{EW}}) = -(312 \text{ MeV})^3. \quad (6)$$

We proceed to fit masses of other pseudoscalar and scalar mesons to data. The minima of  $V_\Sigma$  are numerically

<sup>2</sup> QCD backreaction  $V_h \ni y_q h \langle \bar{q}q \rangle / \sqrt{2}$  is ignored, as it is sizable only for the  $SU(3)_V$  vacuum which is not Hubble selected for  $v_h \lesssim v_h^*$ .

parameter	$f_\pi$	$f_K$	$m_\pi$	$m_K$	$m_\eta$	$m_{\eta'}$	$m_{a_0}$	$m_{f_0(500)}$	$m_{f_0(1370)}$	$m_{K^*(1430)}$
measured	92.4	113	$139.57^{±0.005}$	$497.61^{±0.013}$	$547.86^{±0.017}$	$957.78^{±0.06}$	$980^{±20}$	$500^{±150}$	$1370^{±150}$	$1425^{±50}$
benchmark	92.4	113	137	491	534	973	1050	731	1260	1140

TABLE I. Predictions of the benchmark SM point [Eq. (6) and (7)], compared with data from the Particle Data Group [55]. In units of MeV.

found by considering the stability along all 18 field directions. The  $N_f = 3$  LSM is known to have three types of vacua at  $\mathcal{H} = 0$  [56, 57]:  $SU(3)_L \times SU(3)_R$  ( $s_1 = s_3 = 0$ ),  $SU(3)_V$  ( $s_1 = s_3 \neq 0$ ), and  $SU(2)_L \times SU(2)_R \times U(1)_V$  ( $s_1 = 0, s_3 \neq 0$ ), where  $\langle \Sigma \rangle = \sigma_0 T^0 + \sigma_8 T^8 = \text{diag}(s_1, s_1, s_3)$ . In particular, the global  $SU(3)_V$  vacuum (that we live today) and the local  $SU(3)_L \times SU(3)_R$  vacuum *coexist* if  $\mu^2 > 0$  and  $K \equiv \frac{c^2}{2\mu^2(3\lambda_1 + \lambda_2)} > 4.5$  with  $3\lambda_1 + \lambda_2 > 0$  [57]. Thus, this parameter space is our focus, that potentially exhibits first-order quantum critical points.

By scanning with these constraints, we found a range of good parameter space (see Appendix A in Supplemental Material [58]). The benchmark SM point is [with Eq. (6)]

$$\mu^2 = (60 \text{ MeV})^2, \quad c = 4800 \text{ MeV}, \quad \lambda_1 = 7, \quad \lambda_2 = 46, \quad (7)$$

yielding  $K = 47.8$ . Its goodness of fit to the meson spectrum (Table I) is  $\chi^2/\text{degrees of freedom} = 0.44$  with the first seven observables and 3.11 including all. The first seven are the most reliable, while the last three are less precisely measured with unclear identities [55]. Here, 5% theoretical uncertainties are added as typical sizes of the perturbative corrections. Our benchmark is as good as existing benchmarks in the literature: Ref. [56] (with  $\mu^2 > 0$ ) yielded 0.20 and 2.84, respectively, and Ref. [59] ( $\mu^2 < 0$ ) yielded 1.22 and 4.64.<sup>3</sup> But ours differs in that quantum critical points  $v_h^*$  may exist.

We turn to discuss the vacuum structure away from the SM point for  $v_h < v_{\text{EW}}$ . How does  $V_\Sigma$ , in particular  $\mathcal{H}$ , depend on  $v_h$ ? Since this is not known, we deduce it as follows. The current divergence [Eq. (4)] calculated from QCD or chiral Lagrangian yields  $m_\pi^2 \propto m_q$ , which is also  $\propto h_{0,8}$  from Eq. (5). It suggests  $h_{0,8} \propto v_h$ . Indeed, identifying the  $\mathcal{H}$  term and the current mass term,  $\mathcal{L} \ni -m_q(\bar{u}u + \bar{d}d) - m_s\bar{s}s$ , yields the ratio  $h_8/h_0 \simeq \left(\frac{m_q - m_s}{\sqrt{3}}\right) / \left(\frac{2m_q + m_s}{\sqrt{6}}\right) \simeq -1.3$  using  $m_q = \frac{(m_u + m_d)}{2} = 3.4 \text{ MeV}$  and  $m_s = 93 \text{ MeV}$  [55], same as the ratio from Eq. (6). Thus, we assume that  $\mathcal{H}$  is linear to  $v_h$  as

$$h_{0,8}(v_h) = h_{0,8}(v_{\text{EW}}) \frac{v_h}{v_{\text{EW}}}. \quad (8)$$

Other LSM parameters and dimensionful factors could also depend on  $v_h$ , either directly or indirectly, e.g. via

<sup>3</sup> Large uncertainties of the last three observables allow various good fits; otherwise, the LSM would have been over constrained at the tree level. Higher-order, nonperturbative, and other effects may be calculated by lattice simulations [60–64].

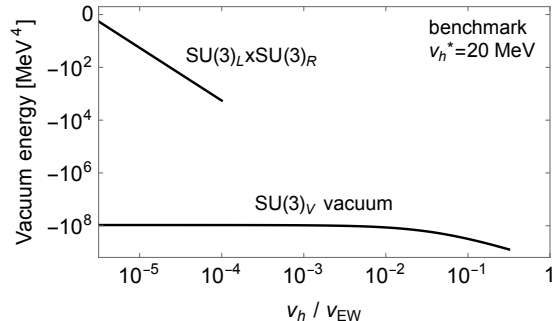


FIG. 1. Vacuum energies of benchmark coexisting QCD vacua at  $T = 0$ , as functions of  $v_h$ . The critical point is at  $v_h^* \simeq 20 \text{ MeV}$ , with a  $\Lambda_{\text{QCD}}$ -scale energy difference.

condensation or  $\Lambda_{\text{QCD}}$ .  $\Lambda_{\text{QCD}}$  depends on quark masses via renormalization running but only logarithmically, and instanton contributions on masses and condensates but complicated and nonperturbative [65]. In this initial exploration, Eq. (8) is assumed to be the only change of  $V_\Sigma$  induced by the scanning of  $v_h$ .

The vacuum structure as a function of  $v_h$  (other parameters fixed to the benchmark) is shown in Fig. 1. As  $K > 4.5$  dictates, there are coexisting vacua at  $v_h = 0$ . As  $v_h$  (hence,  $\mathcal{H}$ ) increases with Eq. (8), and the metastable  $SU(3)_L \times SU(3)_R$  vacuum becomes shallower and unstable at the critical point, which is found at  $v_h^* \simeq 20 \text{ MeV}$ ; in fact, a wider range of  $v_h^* = \mathcal{O}(1 \sim 100) \text{ MeV}$  is consistent with the meson data (see Appendix A in Supplemental Material [58]). The energy difference of the coexisting vacua at the critical point is 93 MeV, comparable to  $\Lambda_{\text{QCD}}$ ; the potential energies are parameterized in Eq. (14) and (15).

In all, we have shown that QCD may possess quantum critical points at  $v_h^* < v_{\text{EW}}$ , which needs dedicated verification.

#### IV. HUBBLE SELECTION

Inflationary quantum fluctuations on the scalar field allow access to a higher potential regime, which is forbidden classically. Although the field in each Hubble patch always rolls down in average, larger Hubble rates at higher potentials can make a difference in the global field-value distribution among patches, culminating in Hubble selection. This section reviews and supplements it [22].

The volume-weighted (global) distribution  $\rho(\phi, t)$  of the field value  $\phi$  obeys the modified Fokker-Planck equa-

tion (FPV) [66–69]

$$\frac{\partial \rho(\phi, t)}{\partial t} = \frac{\partial}{\partial \phi} \left( \frac{V'}{3H} \rho \right) + \frac{1}{8\pi^2} \frac{\partial^2 (H^3 \rho)}{\partial \phi^2} + 3\Delta H \rho. \quad (9)$$

The first two terms represent the flow and diffusion, just as in the original Fokker-Planck equation which averages over Langevin motions. The variation of the Hubble rate  $3\Delta H(\phi) = \frac{V(\phi)}{2M_{\text{Pl}}^2 H_0} \ll 3H_0$  accounts for volume weights within a distribution:  $M_{\text{Pl}} = 2.4 \times 10^{18}$  GeV. The meanings become clearer if we look at a solution (for a linear potential without boundary conditions),

$$\rho(\phi, t) \propto \exp \left\{ \frac{-1}{2\sigma_\phi^2(t)} \left[ \phi - (\phi_0 + \dot{\phi}_c t + \frac{3}{2}(\Delta H)' \sigma_\phi^2 t) \right]^2 \right\}, \quad (10)$$

where the exponent describes the motion of a peak.  $\dot{\phi}_c = -V'/3H$  is classical rolling. Remarkably, an additional velocity  $\dot{\phi}_H = 3(\Delta H)' \sigma_\phi(t)^2$  with opposite sign arises from volume weights within the width  $\sigma_\phi$ , which grows in the beginning of FPV evolutions due to quantum diffusion  $\sigma_\phi^2(t) = (\frac{H}{2\pi})^2 H t$  from the de Sitter temperature  $H/2\pi$  [70, 71].

“Hubble selection” starts to operate when the peak of a distribution starts to *climb up* the potential:  $\sigma_\phi^2 \simeq \frac{2}{3} M_{\text{Pl}}^2$ . The width at this moment is always Planckian, reflecting its quantum nature. The field excursion by this moment is non-negligible,  $\Delta\phi \sim \frac{4\pi^2 M_{\text{Pl}} \Lambda_\phi^4}{9 H^4 M^2/g}$ . Thus, for a peak to climb, the field range  $\delta\phi \sim M^2/g$  (needed to scan  $\mu_h^2$  up to  $M^2$ ) must accommodate both the field excursion  $\Delta\phi$  (stronger condition) and width  $\sigma_\phi$ , yielding respectively

$$g \lesssim H \frac{H}{M_{\text{Pl}}} \frac{M^2}{\Lambda_\phi^2} \lesssim \frac{M^2}{M_{\text{Pl}}}. \quad (11)$$

We call this condition *global* quantum beats classical (QBC). It is stronger than the usual local QBC,  $V' \lesssim H^3$ , requiring  $g \lesssim H \frac{H^2}{\Lambda_\phi^2} \frac{M^2}{\Lambda_\phi^2}$ , because  $\Lambda_\phi^2 \lesssim H M_{\text{Pl}}$  from condition 1 later. It also has different meanings as it involves the field range while the local one depends only on the potential slope. It turns out to be equivalent to the Quantum+Volume (QV) condition in Ref. [22] (see Appendix B in Supplemental Material [58]) which also accounted for volume effects. If it is not satisfied,  $\rho$  makes an equilibrium at the bottom of a potential, but with the sub-Planckian width consistently  $\sigma_\phi \sim H^2/m_\phi \sim H^2 M^2/\Lambda_\phi^2 g \lesssim M_{\text{Pl}}$  [72, 73]. Thus, we require the global QBC Eq. (11) for Hubble selection.

The e-folding until this moment  $\Delta N \simeq \frac{8\pi^2 M_{\text{Pl}}^2}{3H^2}$  already saturates the upper bound for finite inflation,  $\frac{2\pi^2 M_{\text{Pl}}^2}{3H^2}$ , given by the de Sitter entropy [74–76]. Thus, Hubble selection needs eternal inflation, and the universe eventually reaches a stationary state [77–80]. Probability distributions are to be defined within an ensemble of Hubble

patches that have reached reheating [81–83]. As the latter patches dominate the ensemble with an exponentially larger number, only stationary or equilibrium distributions matter; for landscapes, this can be different [84–87].

$\rho(\phi, t)$  makes an equilibrium somewhere near the top of a potential, which is the critical point  $\phi_*$  in this work. The distribution can be especially narrow [Planckian in the global QBC regime; see Eq.(B6) in Supplemental Material [58]] if energy drops sharply after  $\phi_*$ . This is how Hubble selection self-organizes the universe toward critical points [22].

The flatter the potential is (with stronger quantum effects), the closer to  $\phi_*$  is the equilibrium. The closest possible field distance is Planckian, again reflecting the uncertainty principle. For even flatter potentials, the equilibrium distribution rather spreads away from  $\phi_*$ , because distributions will be flat in the limit  $V' \rightarrow 0$ . The equilibrium near  $\phi_*$  is estimated as follows. The boundary condition  $\rho(\phi \geq \phi_*) = 0$  (discarding Hubble patches with  $\phi \geq \phi_*$ ) induces repulsive motion  $\dot{\phi}_b \sim -H^3/(8\pi^2 \sigma_\phi)$  [? ], so that the balance requires  $\dot{\phi}_c + \dot{\phi}_H + \dot{\phi}_b \simeq 0$ . When  $\dot{\phi}_b \gg \dot{\phi}_c$ , an equilibrium is reached with

$$\sigma_\phi \simeq \left( \frac{M_{\text{Pl}}^2 H^4}{4\pi^2 V'} \right)^{1/3} \simeq \left( \frac{M_{\text{Pl}}^2 M^2 H^4}{4\pi^2 g \Lambda_\phi^4} \right)^{1/3}, \quad (12)$$

which is the width in the Quantum<sup>2</sup>+Volume (Q<sup>2</sup>V) regime [22]. The width indeed increases as  $V$  flattens; nevertheless, the  $v_h$  distribution can be arbitrarily narrowed, as will be discussed. One also expects  $|\phi_{\text{peak}} - \phi_*| \sim \sigma_\phi$  from dimensional ground. These heuristic discussions on Q<sup>2</sup>V are demonstrated with the method of images in Appendix B of Supplemental Material [58].

A theory enters the Q<sup>2</sup>V regime when the balance width becomes larger than  $M_{\text{Pl}}$  (the width in the global QBC):

$$g \lesssim H \frac{H}{M_{\text{Pl}}} \frac{H^2 M^2}{\Lambda_\phi^4}. \quad (13)$$

This is equivalent to  $V' \lesssim H^3 H/M_{\text{Pl}}$  [22], which is also derived from the local balance near  $\phi_*$ . Q<sup>2</sup>V is typically stronger than the global QBC and not absolutely needed for Hubble selection, but later will be useful for efficient localization of  $v_h$ .

## V. THE WEAK SCALE CRITICALITY

Finally, we come to calculate the equilibrium distribution of  $\rho(v_h)$  in our model. We first discuss conditions for the successful Hubble selection of  $v_h^*$ , and then present benchmark results.

The scanning of  $v_h$  starts by  $\phi$  rolling up its potential from  $\phi < 0$  to  $> 0$ . When  $\phi < 0$  ( $\mu_h^2 > 0$ ),  $v_h = 0$  and  $V_h = V_\Sigma = 0$  remain unchanged with  $\phi$ . Thus  $\phi$  simply keeps growing, driven by quantum effects. The

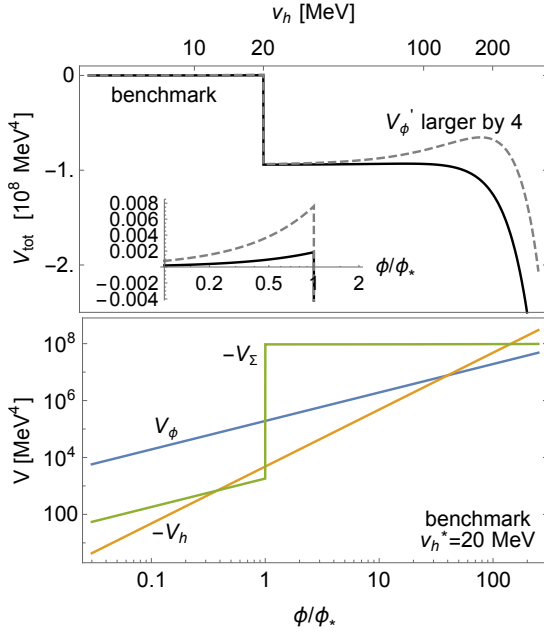


FIG. 2. Top: Total potential energy near the critical point as a function of  $\phi$ , for the benchmark Eq. (18); dashed line for comparison. Inset: Zoom-in near  $\phi_*$ . Bottom: Individual contribution from  $V_\phi$ ,  $|V_\Sigma|$ , and  $|V_h|$ .

only constraint is that  $V_\phi$  must not affect the inflation dynamics (condition 1):  $\Lambda_\phi^4 \lesssim H^2 M_{\text{Pl}}^2$ .

As soon as  $\phi > 0$  ( $\mu_h^2 \leq 0$ ), the Higgs gets the vacuum expectation value  $v_h > 0$ , and  $V_h$ ,  $V_\Sigma$  minima now evolve with  $\phi$ .  $V_h = -\frac{\lambda_h}{4} v_h^4$ , and coexisting vacua of  $V_\Sigma$  are, at leading orders in  $v_h$ ,

$$V_{\Sigma(L \times R)} \simeq -a_1 \Lambda_{\text{QCD}}^4 \frac{v_h^2}{v_{\text{EW}}^2}, \quad (14)$$

$$V_{\Sigma(V)} \simeq -\Lambda_{\text{QCD}}^4 (a_2 + a_3 \frac{v_h}{v_{\text{EW}}}), \quad (15)$$

where  $a_1 \simeq 114$ ,  $a_2 \simeq 0.059$ ,  $a_3 \simeq 1.38$  for the benchmark (Fig. 1).  $\langle \sigma_0 \rangle_{(L \times R)} \simeq -\langle \sigma_8 \rangle \simeq a_4 v_h$  with  $a_4 \simeq 0.025$ . Note that  $V_{h,\Sigma}$  decrease with  $\phi$ , which must be slower than the increase of  $V_\phi \simeq \frac{g \Lambda_\phi^4}{M^2} \phi$ , for Hubble selection.

Which potential dominates the  $\phi$  dynamics? Fig. 2 shows individual potential with  $\phi$ , whose slope is

$$\frac{\delta V_\phi}{\delta \phi} \sim g \frac{\Lambda_\phi^4}{M^2}, \quad \frac{\delta V_{\Sigma(L \times R)}}{\delta \phi} \sim -a_1 \frac{g}{\lambda_h} \frac{\Lambda_{\text{QCD}}^4}{v_{\text{EW}}^2}, \quad (16)$$

$$\frac{\delta V_h}{\delta \phi} \sim -\frac{g}{2} v_h^2, \quad \frac{\delta V_{\Sigma(V)}}{\delta \phi} \sim -a_3 \frac{g}{\lambda_h} \frac{\Lambda_{\text{QCD}}^4}{v_h v_{\text{EW}}}.$$

The dominance of growing  $\delta V_\phi / \delta \phi$  up to  $v_h \leq v_h^*$  requires  $\Lambda_\phi^2 / M \gtrsim v_h^*$ , unless  $v_h$  is too small. After  $\Lambda_{\text{QCD}}$ -scale energy drops in  $V_\Sigma$  at  $v_h^*$ , dominant  $V_\phi$  keeps growing. For large enough  $v_h \gtrsim \Lambda_{\text{QCD}} (\gtrsim v_h^*)$ , decreasing  $V_h$  begins to dominate and is prohibited from being Hubble selected again. So we need to make sure that  $V_\phi$  never compensates the energy drop in the intermediate region

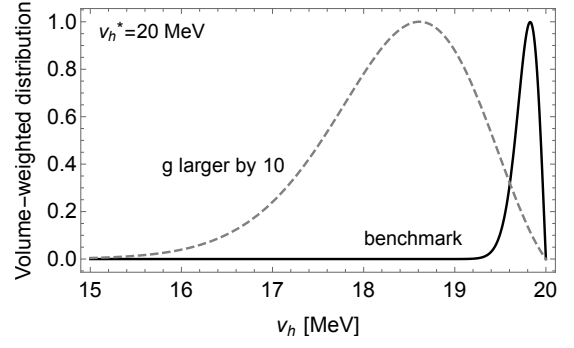


FIG. 3. The probability distribution of  $v_h$  among Hubble patches that have reached reheating.  $\sigma_{v_h} \simeq 0.1 \text{ MeV} \ll v_h^*$  for the benchmark Eq. (18); dashed line for comparison.

$v_h^* \lesssim v_h \lesssim \Lambda_{\text{QCD}}$ :  $\Delta V_\phi \simeq \frac{g \Lambda_\phi^4}{M^2} \frac{\lambda_h \Lambda_{\text{QCD}}^2}{g} \lesssim \Lambda_{\text{QCD}}^4$ . In all,  $V_\phi$  cannot be too flat or too steep (condition 2):

$$v_h^* \lesssim \Lambda_\phi^2 / M \lesssim \Lambda_{\text{QCD}}. \quad (17)$$

In addition,  $h$  and  $\Sigma$  are required to sit in their respective minima, not quantum driven to overflow their potentials. Their equilibrium widths must be small enough:  $H^2 / m_{h,\Sigma} \lesssim \Lambda_{\text{QCD}}$ , with  $m_h \sim v_h$  and  $m_\Sigma \sim \Lambda_{\text{QCD}}$  in the higher-energy  $SU(3)_L \times SU(3)_R$  vacuum. Since  $v_h^* \lesssim \Lambda_{\text{QCD}}$  from condition 2, we obtain (condition 3):  $H \lesssim v_h^*$ .

For numerical studies, we use the following benchmark ( $v_h^*$  from Sec. III),

$$v_h^* \simeq 20 \text{ MeV}, \quad H = v_h^*, \quad M = 3 \times 10^{-3} M_{\text{Pl}}, \\ \Lambda_\phi^2 = 10^{-2} H M_{\text{Pl}}, \quad g = 10^{-3} H^2 / M_{\text{Pl}}, \quad (18)$$

satisfying the global QBC [Eq. (11)] (and Q<sup>2</sup>V [Eq. (13)] marginally) and conditions 1–3. Potential energies near  $v_h^*$  are shown in Fig. 2. As desired, the total energy peaks sharply at  $v_h^*$ , drops significantly, and is never compensated afterwards; for much smaller or larger  $V_\phi'$ , energy would not sharply peak.

The large-time equilibrium distribution of  $v_h$  is shown in Fig. 3; see Appendix C in Supplemental Material [58] for details. The width  $\sigma_{v_h}$  is translated from  $\sigma_\phi$  via  $v_h^2 = g\phi / \lambda_h$  as

$$\sigma_{v_h} \simeq \frac{g \sigma_\phi}{2 \lambda_h v_h^*}, \quad (19)$$

where  $\sigma_\phi \simeq 1.3 M_{\text{Pl}}$  from Eq. (12) for the benchmark with marginal Q<sup>2</sup>V.<sup>4</sup> Thus we have  $\sigma_{v_h} \simeq 0.1 \text{ MeV} \ll v_h^*$ , which is narrow enough so that most Hubble patches self-organize to have  $v_h \approx v_h^*$  ( $\sim v_{\text{EW}}$ ). Note that it can be

<sup>4</sup> The Planckian width is a generic result of the global QBC,  $\sigma_\phi \simeq \phi_* \left( \frac{3 \phi_*^2}{2 M_{\text{Pl}}^2} \right)^{-1/2} \sim M_{\text{Pl}}$ ; see Eq. (B6) in Supplemental Material [58].

arbitrarily narrower at the price of arbitrarily smaller  $g$  or larger  $\phi$  range, moving into a deeper  $Q^2V$  regime; only the resulting hierarchy  $f_\phi = M^2/g \gg M_{\text{Pl}}$  needs to be generated consistently in field theory [46–48]. On the other limit, unwanted  $\sigma_{v_h} \gtrsim v_h^*$  is resulted for 10–100 times larger  $g$ , where  $Q^2V$  is not even marginally satisfied.

Postinflationary dynamics is model dependent but such that  $\phi$  slow rolls to the today’s  $v_{\text{EW}}$ . Today,  $\phi$  could be still safely slow rolling or trapped by SM back-reactions. Signals from time-dependent  $v_h$  or phase transitions could be produced.

## VI. DISCUSSION

In this Letter, we have discussed the self-organized criticality of the weak scale, by exploiting possible first-order quantum critical points of QCD. Although we saw some success, our exploration of critical points is much simplified and far from conclusive. We have used only LSM with  $N_f = 3$  at the tree level with a simplified dependence on  $v_h \leq v_{\text{EW}}$  in Eq. (8). They shall be verified and generalized by lattice calculations [36–43], incorporating higher-order and nonperturbative effects [60–64], not only for the SM point but also away from it with  $v_h \leq v_{\text{EW}}$ .  $N_f > 3$  likely yields a richer vacuum structure but needs a dedicated calculation. Theoretical intuitions from confining gauge theories might also be useful.

If such a critical point is indeed built in QCD, it would shed significant light on the role of near criticality of the SM.

The proposed scenario makes an advancement on the hierarchy problem, albeit not yet completely solving it. It is not complete because Hubble selection requires a mild separation of scales  $\Lambda_\phi \ll M$  from Eq. (17) (if  $M \sim \Lambda_\phi$  strictly,  $M \lesssim \Lambda_{\text{QCD}}$  is too low) but this is not quantum stable (Higgs loop diagrams with external relaxation legs yield  $\Lambda_\phi \sim \text{cutoff } M$  [4, 47]). Thus, a little hierarchy remains; with the fine-tuning  $\epsilon \equiv \Lambda_\phi/M < 1$ , the cutoff can be as high as  $M \lesssim \Lambda_{\text{QCD}}/\epsilon^2$ . Another advancement is that choosing  $\Lambda_\phi$  can be translated to a dynamical problem of choosing dimensionless parameters of the extended relaxation sector, such as in Ref. [4]. Further explorations will be enlightening.

The near criticality and naturalness of nature may be intimately connected by quantum cosmology, with necessary criticality perhaps built in just around the SM. Further theoretical and experimental studies are encouraged to unveil this connection.

## ACKNOWLEDGMENTS

We thank Sang Hui Im, Hyung Do Kim, Choonkyu Lee, and Ke-Pan Xie for valuable conversations. We are supported by National Research Foundation of Korea under Grant No. NRF-2019R1C1C1010050, and S.J. also by a POSCO Science Fellowship.

- 
- [1] G. F. Giudice and R. Rattazzi, “Living Dangerously with Low-Energy Supersymmetry,” *Nucl. Phys. B* **757** (2006), 19-46 doi:10.1016/j.nuclphysb.2006.07.031 [arXiv:hep-ph/0606105 [hep-ph]].
  - [2] G. F. Giudice, “Naturally Speaking: The Naturalness Criterion and Physics at the LHC,” doi:10.1142/9789812779762\_0010 [arXiv:0801.2562 [hep-ph]].
  - [3] P. W. Graham, D. E. Kaplan and S. Rajendran, “Cosmological Relaxation of the Electroweak Scale,” *Phys. Rev. Lett.* **115**, no.22, 221801 (2015) doi:10.1103/PhysRevLett.115.221801 [arXiv:1504.07551 [hep-ph]].
  - [4] J. R. Espinosa, C. Grojean, G. Panico, A. Pomarol, O. Pujolàs and G. Servant, “Cosmological Higgs-Axion Interplay for a Naturally Small Electroweak Scale,” *Phys. Rev. Lett.* **115**, no.25, 251803 (2015) doi:10.1103/PhysRevLett.115.251803 [arXiv:1506.09217 [hep-ph]].
  - [5] T. You, “A Dynamical Weak Scale from Inflation,” *JCAP* **09** (2017), 019 doi:10.1088/1475-7516/2017/09/019 [arXiv:1701.09167 [hep-ph]].
  - [6] M. Geller, Y. Hochberg and E. Kuflik, “Inflating to the Weak Scale,” *Phys. Rev. Lett.* **122**, no.19, 191802 (2019) doi:10.1103/PhysRevLett.122.191802 [arXiv:1809.07338 [hep-ph]].
  - [7] C. Cheung and P. Saraswat, “Mass Hierarchy and Vacuum Energy,” [arXiv:1811.12390 [hep-ph]].
  - [8] N. Arkani-Hamed, R. T. D’Agnolo and H. D. Kim, “Weak scale as a trigger,” *Phys. Rev. D* **104**, no.9, 095014 (2021) doi:10.1103/PhysRevD.104.095014 [arXiv:2012.04652 [hep-ph]].
  - [9] G. Degrandi, S. Di Vita, J. Elias-Miro, J. R. Espinosa, G. F. Giudice, G. Isidori and A. Strumia, “Higgs mass and vacuum stability in the Standard Model at NNLO,” *JHEP* **08** (2012), 098 doi:10.1007/JHEP08(2012)098 [arXiv:1205.6497 [hep-ph]].
  - [10] D. Buttazzo, G. Degrandi, P. P. Giardino, G. F. Giudice, F. Sala, A. Salvio and A. Strumia, “Investigating the near-criticality of the Higgs boson,” *JHEP* **12** (2013), 089 doi:10.1007/JHEP12(2013)089 [arXiv:1307.3536 [hep-ph]].
  - [11] C. D. Froggatt and H. B. Nielsen, “Standard model criticality prediction: Top mass 173 +- 5-GeV and Higgs mass 135 +- 9-GeV,” *Phys. Lett. B* **368**, 96-102 (1996) doi:10.1016/0370-2693(95)01480-2 [arXiv:hep-ph/9511371 [hep-ph]].
  - [12] C. D. Froggatt, H. B. Nielsen and Y. Takahashi, “Standard model Higgs boson mass from borderline metastability of the vacuum,” *Phys. Rev. D* **64**, 113014 (2001) doi:10.1103/PhysRevD.64.113014 [arXiv:hep-ph/0104161 [hep-ph]].

- [13] H. Kawai, “Low energy effective action of quantum gravity and the naturalness problem,” *Int. J. Mod. Phys. A* **28**, 1340001 (2013) doi:10.1142/S0217751X13400010
- [14] Y. Hamada, H. Kawai and K. Kawana, “Natural solution to the naturalness problem: The universe does fine-tuning,” *PTEP* **2015**, no.12, 123B03 (2015) doi:10.1093/ptep/ptv168 [arXiv:1509.05955 [hep-th]].
- [15] H. Kawai and K. Kawana, “The multicritical point principle as the origin of classical conformality and its generalizations,” *PTEP* **2022**, no.1, 013B11 (2022) doi:10.1093/ptep/ptab161 [arXiv:2107.10720 [hep-th]].
- [16] E. J. Chun, S. Jung and H. M. Lee, “Radiative generation of the Higgs potential,” *Phys. Lett. B* **725**, 158-163 (2013) [erratum: *Phys. Lett. B* **730**, 357-359 (2014)] doi:10.1016/j.physletb.2013.06.055 [arXiv:1304.5815 [hep-ph]].
- [17] D. Chway, T. H. Jung, H. D. Kim and R. Dermisek, “Radiative Electroweak Symmetry Breaking Model Perturbative All the Way to the Planck Scale,” *Phys. Rev. Lett.* **113**, no.5, 051801 (2014) doi:10.1103/PhysRevLett.113.051801 [arXiv:1308.0891 [hep-ph]].
- [18] M. Hashimoto, S. Iso and Y. Orikasa, “Radiative symmetry breaking at the Fermi scale and flat potential at the Planck scale,” *Phys. Rev. D* **89**, no.1, 016019 (2014) doi:10.1103/PhysRevD.89.016019 [arXiv:1310.4304 [hep-ph]].
- [19] F. L. Bezrukov and M. Shaposhnikov, “The Standard Model Higgs boson as the inflaton,” *Phys. Lett. B* **659**, 703-706 (2008) doi:10.1016/j.physletb.2007.11.072 [arXiv:0710.3755 [hep-th]].
- [20] Y. Hamada, H. Kawai and K. y. Oda, “Minimal Higgs inflation,” *PTEP* **2014**, 023B02 (2014) doi:10.1093/ptep/ptt116 [arXiv:1308.6651 [hep-ph]].
- [21] Y. Hamada, H. Kawai, K. y. Oda and S. C. Park, “Higgs inflation from Standard Model criticality,” *Phys. Rev. D* **91**, 053008 (2015) doi:10.1103/PhysRevD.91.053008 [arXiv:1408.4864 [hep-ph]].
- [22] G. F. Giudice, M. McCullough and T. You, “Self-organised localisation,” *JHEP* **10**, 093 (2021) doi:10.1007/JHEP10(2021)093 [arXiv:2105.08617 [hep-ph]].
- [23] G. Kartvelishvili, J. Khoury and A. Sharma, “The Self-Organized Critical Multiverse,” *JCAP* **02**, 028 (2021) doi:10.1088/1475-7516/2021/02/028 [arXiv:2003.12594 [hep-th]].
- [24] J. Khoury and O. Parrikar, “Search Optimization, Funnel Topography, and Dynamical Criticality on the String Landscape,” *JCAP* **12**, 014 (2019) doi:10.1088/1475-7516/2019/12/014 [arXiv:1907.07693 [hep-th]].
- [25] G. F. Giudice, A. Kehagias and A. Riotto, “The Selfish Higgs,” *JHEP* **10** (2019), 199 doi:10.1007/JHEP10(2019)199 [arXiv:1907.05370 [hep-ph]].
- [26] A. Strumia and D. Teresi, “Relaxing the Higgs mass and its vacuum energy by living at the top of the potential,” *Phys. Rev. D* **101** (2020) no.11, 115002 doi:10.1103/PhysRevD.101.115002 [arXiv:2002.02463 [hep-ph]].
- [27] C. Csáki, R. T. D’Agnolo, M. Geller and A. Ismail, “Crunching Dilaton, Hidden Naturalness,” *Phys. Rev. Lett.* **126** (2021), 091801 doi:10.1103/PhysRevLett.126.091801 [arXiv:2007.14396 [hep-ph]].
- [28] R. Tito D’Agnolo and D. Teresi, “Sliding Naturalness: New Solution to the Strong- $CP$  and Electroweak-Hierarchy Problems,” *Phys. Rev. Lett.* **128**, no.2, 021803 (2022) doi:10.1103/PhysRevLett.128.021803 [arXiv:2106.04591 [hep-ph]].
- [29] R. Tito D’Agnolo and D. Teresi, “Sliding Naturalness: Cosmological Selection of the Weak Scale,” [arXiv:2109.13249 [hep-ph]].
- [30] G. Dvali and A. Vilenkin, “Cosmic attractors and gauge hierarchy,” *Phys. Rev. D* **70** (2004), 063501 doi:10.1103/PhysRevD.70.063501 [arXiv:hep-th/0304043 [hep-th]].
- [31] G. Dvali, “Large hierarchies from attractor vacua,” *Phys. Rev. D* **74** (2006), 025018 doi:10.1103/PhysRevD.74.025018 [arXiv:hep-th/0410286 [hep-th]].
- [32] H. Kawai and T. Okada, “Solving the Naturalness Problem by Baby Universes in the Lorentzian Multiverse,” *Prog. Theor. Phys.* **127**, 689-721 (2012) doi:10.1143/PTP.127.689 [arXiv:1110.2303 [hep-th]].
- [33] Y. Hamada, H. Kawai and K. Kawana, “Weak Scale From the Maximum Entropy Principle,” *PTEP* **2015**, 033B06 (2015) doi:10.1093/ptep/ptv011 [arXiv:1409.6508 [hep-ph]].
- [34] N. Arkani-Hamed, T. Cohen, R. T. D’Agnolo, A. Hook, H. D. Kim and D. Pinner, “Solving the Hierarchy Problem at Reheating with a Large Number of Degrees of Freedom,” *Phys. Rev. Lett.* **117** (2016) no.25, 251801 doi:10.1103/PhysRevLett.117.251801 [arXiv:1607.06821 [hep-ph]].
- [35] A. Arvanitaki, S. Dimopoulos, V. Gorbenko, J. Huang and K. Van Tilburg, “A small weak scale from a small cosmological constant,” *JHEP* **05** (2017), 071 doi:10.1007/JHEP05(2017)071 [arXiv:1609.06320 [hep-ph]].
- [36] F. R. Brown, F. P. Butler, H. Chen, N. H. Christ, Z. h. Dong, W. Schaffer, L. I. Unger and A. Vaccarino, “On the existence of a phase transition for QCD with three light quarks,” *Phys. Rev. Lett.* **65**, 2491-2494 (1990) doi:10.1103/PhysRevLett.65.2491
- [37] S. Gavin, A. Gocksch and R. D. Pisarski, “QCD and the chiral critical point,” *Phys. Rev. D* **49**, R3079-R3082 (1994) doi:10.1103/PhysRevD.49.R3079 [arXiv:hep-ph/9311350 [hep-ph]].
- [38] C. DeTar and U. M. Heller, “QCD Thermodynamics from the Lattice,” *Eur. Phys. J. A* **41**, 405-437 (2009) doi:10.1140/epja/i2009-10825-3 [arXiv:0905.2949 [hep-lat]].
- [39] P. de Forcrand and M. D’Elia, “Continuum limit and universality of the Columbia plot,” *PoS LATTICE2016*, 081 (2017) doi:10.22323/1.256.0081 [arXiv:1702.00330 [hep-lat]].
- [40] S. T. Li and H. T. Ding, “Chiral phase transition of  $(2 + 1)$ -flavor QCD on  $N_\tau = 6$  lattices,” *PoS LATTICE2016*, 372 (2017) doi:10.22323/1.256.0372 [arXiv:1702.01294 [hep-lat]].
- [41] F. Cuteri, C. Czaban, O. Philipsen and A. Sciarra, “Updates on the Columbia plot and its extended/alternative versions,” *EPJ Web Conf.* **175**, 07032 (2018) doi:10.1051/epjconf/201817507032 [arXiv:1710.09304 [hep-lat]].
- [42] S. Resch, F. Rennecke and B. J. Schaefer, “Mass sensitivity of the three-flavor chiral phase transition,” *Phys. Rev. D* **99**, no.7, 076005 (2019)

- doi:10.1103/PhysRevD.99.076005 [arXiv:1712.07961 [hep-ph]].
- [43] Y. Kuramashi, Y. Nakamura, H. Ohno and S. Takeda, “Nature of the phase transition for finite temperature  $N_f = 3$  QCD with nonperturbatively  $O(a)$  improved Wilson fermions at  $N_t = 12$ ,” *Phys. Rev. D* **101**, no.5, 054509 (2020) doi:10.1103/PhysRevD.101.054509 [arXiv:2001.04398 [hep-lat]].
- [44] R. D. Pisarski and F. Wilczek, “Remarks on the Chiral Phase Transition in Chromodynamics,” *Phys. Rev. D* **29**, 338-341 (1984) doi:10.1103/PhysRevD.29.338
- [45] F. Wilczek, “Application of the renormalization group to a second order QCD phase transition,” *Int. J. Mod. Phys. A* **7**, 3911-3925 (1992) [erratum: *Int. J. Mod. Phys. A* **7**, 6951 (1992)] doi:10.1142/S0217751X92001757
- [46] J. E. Kim, H. P. Nilles and M. Peloso, “Completing natural inflation,” *JCAP* **01**, 005 (2005) doi:10.1088/1475-7516/2005/01/005 [arXiv:hep-ph/0409138 [hep-ph]].
- [47] K. Choi and S. H. Im, “Realizing the relaxation from multiple axions and its UV completion with high scale supersymmetry,” *JHEP* **01**, 149 (2016) doi:10.1007/JHEP01(2016)149 [arXiv:1511.00132 [hep-ph]].
- [48] D. E. Kaplan and R. Rattazzi, “Large field excursions and approximate discrete symmetries from a clockwork axion,” *Phys. Rev. D* **93**, no.8, 085007 (2016) doi:10.1103/PhysRevD.93.085007 [arXiv:1511.01827 [hep-ph]].
- [49] M. Gell-Mann and M. Levy, “The axial vector current in beta decay,” *Nuovo Cim.* **16**, 705 (1960) doi:10.1007/BF02859738
- [50] M. Levy, “Current and Symmetry Breaking,” *Nuovo Cim.* **52**, 23 (1967) doi:10.1007/BF02739271
- [51] B. W. Lee, “Chiral Dynamics,” *Gordon and Breach* (1972)
- [52] G. 't Hooft, “Symmetry Breaking Through Bell-Jackiw Anomalies,” *Phys. Rev. Lett.* **37**, 8-11 (1976) doi:10.1103/PhysRevLett.37.8
- [53] G. 't Hooft, “Computation of the Quantum Effects Due to a Four-Dimensional Pseudoparticle,” *Phys. Rev. D* **14**, 3432-3450 (1976) [erratum: *Phys. Rev. D* **18**, 2199(E) (1978)] doi:10.1103/PhysRevD.14.3432
- [54] G. Fejos and A. Hosaka, “Thermal properties and evolution of the  $U_A(1)$  factor for 2+1 flavors,” *Phys. Rev. D* **94**, no.3, 036005 (2016) doi:10.1103/PhysRevD.94.036005 [arXiv:1604.05982 [hep-ph]].
- [55] P.A. Zyla *et al.* [Particle Data Group], “Review of Particle Physics,” *PTEP* **2020**, no.8, 083C01 (2020) doi:10.1093/ptep/ptaa104
- [56] J. T. Lenaghan, D. H. Rischke and J. Schaffner-Bielich, “Chiral symmetry restoration at nonzero temperature in the  $SU(3)(r) \times SU(3)(l)$  linear sigma model,” *Phys. Rev. D* **62**, 085008 (2000) doi:10.1103/PhysRevD.62.085008 [arXiv:nucl-th/0004006 [nucl-th]].
- [57] Y. Bai and B. A. Dobrescu, “Minimal  $SU(3) \times SU(3)$  Symmetry Breaking Patterns,” *Phys. Rev. D* **97**, no.5, 055024 (2018) doi:10.1103/PhysRevD.97.055024 [arXiv:1710.01456 [hep-ph]].
- [58] See Supplemental Material for our search results of quantum critical points  $v_h^*$  in the three-flavor LSM (Appendix A), for the properties and derivations of Hubble selection in the quantum regime (Appendix B), and for technical descriptions of our numerical calculations of the equilibrium distribution (Appendix C).
- [59] H. Meyer-Ortmanns and B. J. Schaefer, “How sharp is the chiral crossover phenomenon for realistic meson masses?,” *Phys. Rev. D* **53**, 6586-6601 (1996) doi:10.1103/PhysRevD.53.6586 [arXiv:hep-ph/9409430 [hep-ph]].
- [60] D. J. Gross, R. D. Pisarski and L. G. Yaffe, “QCD and Instantons at Finite Temperature,” *Rev. Mod. Phys.* **53**, 43 (1981) doi:10.1103/RevModPhys.53.43
- [61] J. M. Pawłowski, “Exact flow equations and the  $U(1)$  problem,” *Phys. Rev. D* **58**, 045011 (1998) doi:10.1103/PhysRevD.58.045011 [arXiv:hep-th/9605037 [hep-th]].
- [62] M. Heller and M. Mitter, “Pion and  $\eta$ -meson mass splitting at the two-flavour chiral crossover,” *Phys. Rev. D* **94**, no.7, 074002 (2016) doi:10.1103/PhysRevD.94.074002 [arXiv:1512.05241 [hep-ph]].
- [63] N. Dupuis, L. Canet, A. Eichhorn, W. Metzner, J. M. Pawłowski, M. Tissier and N. Wschebor, “The nonperturbative functional renormalization group and its applications,” *Phys. Rept.* **910**, 1-114 (2021) doi:10.1016/j.physrep.2021.01.001 [arXiv:2006.04853 [cond-mat.stat-mech]].
- [64] J. Braun *et al.* [QCD], “Chiral and effective  $U(1)_A$  symmetry restoration in QCD,” [arXiv:2012.06231 [hep-ph]].
- [65] T. Schäfer and E. V. Shuryak, “Instantons in QCD,” *Rev. Mod. Phys.* **70**, 323-426 (1998) doi:10.1103/RevModPhys.70.323 [arXiv:hep-ph/9610451 [hep-ph]].
- [66] K. i. Nakao, Y. Nambu and M. Sasaki, “Stochastic Dynamics of New Inflation,” *Prog. Theor. Phys.* **80**, 1041 (1988) doi:10.1143/PTP.80.1041
- [67] M. Sasaki, Y. Nambu and K. i. Nakao, “The Condition for Classical Slow Rolling in New Inflation,” *Phys. Lett. B* **209**, 197-202 (1988) doi:10.1016/0370-2693(88)90932-X
- [68] M. Mijic, “Random Walk After the Big Bang,” *Phys. Rev. D* **42**, 2469-2482 (1990) doi:10.1103/PhysRevD.42.2469
- [69] A. D. Linde and A. Mezhlumian, “Stationary universe,” *Phys. Lett. B* **307**, 25-33 (1993) doi:10.1016/0370-2693(93)90187-M [arXiv:gr-qc/9304015 [gr-qc]].
- [70] G. W. Gibbons and S. W. Hawking, “Cosmological Event Horizons, Thermodynamics, and Particle Creation,” *Phys. Rev. D* **15**, 2738-2751 (1977) doi:10.1103/PhysRevD.15.2738
- [71] A. A. Starobinsky and J. Yokoyama, “Equilibrium state of a selfinteracting scalar field in the De Sitter background,” *Phys. Rev. D* **50**, 6357-6368 (1994) doi:10.1103/PhysRevD.50.6357 [arXiv:astro-ph/9407016 [astro-ph]].
- [72] P. W. Graham and A. Scherlis, “Stochastic axion scenario,” *Phys. Rev. D* **98**, no.3, 035017 (2018) doi:10.1103/PhysRevD.98.035017 [arXiv:1805.07362 [hep-ph]].
- [73] F. Takahashi, W. Yin and A. H. Guth, “QCD axion window and low-scale inflation,” *Phys. Rev. D* **98**, no.1, 015042 (2018) doi:10.1103/PhysRevD.98.015042 [arXiv:1805.08763 [hep-ph]].
- [74] N. Arkani-Hamed, S. Dubovsky, A. Nicolis, E. Trincherini and G. Villadoro, “A Measure of de Sitter entropy and eternal inflation,” *JHEP* **05**, 055 (2007) doi:10.1088/1126-6708/2007/05/055 [arXiv:0704.1814 [hep-th]].



- [75] S. Dubovsky, L. Senatore and G. Villadoro, “The Volume of the Universe after Inflation and de Sitter Entropy,” *JHEP* **04**, 118 (2009) doi:10.1088/1126-6708/2009/04/118 [arXiv:0812.2246 [hep-th]].
- [76] S. Dubovsky, L. Senatore and G. Villadoro, “Universality of the Volume Bound in Slow-Roll Eternal Inflation,” *JHEP* **05**, 035 (2012) doi:10.1007/JHEP05(2012)035 [arXiv:1111.1725 [hep-th]].
- [77] M. Aryal and A. Vilenkin, “The Fractal Dimension of Inflationary Universe,” *Phys. Lett. B* **199**, 351-357 (1987) doi:10.1016/0370-2693(87)90932-4
- [78] Y. Nambu, “Stochastic Dynamics of an Inflationary Model and Initial Distribution of Universes,” *Prog. Theor. Phys.* **81**, 1037 (1989) doi:10.1143/PTP.81.1037
- [79] A. D. Linde, D. A. Linde and A. Mezhlumian, “From the Big Bang theory to the theory of a stationary universe,” *Phys. Rev. D* **49**, 1783-1826 (1994) doi:10.1103/PhysRevD.49.1783 [arXiv:gr-qc/9306035 [gr-qc]].
- [80] J. Garcia-Bellido and A. D. Linde, “Stationarity of inflation and predictions of quantum cosmology,” *Phys. Rev. D* **51**, 429-443 (1995) doi:10.1103/PhysRevD.51.429 [arXiv:hep-th/9408023 [hep-th]].
- [81] A. Vilenkin, “Making predictions in eternally inflating universe,” *Phys. Rev. D* **52**, 3365-3374 (1995) doi:10.1103/PhysRevD.52.3365 [arXiv:gr-qc/9505031 [gr-qc]].
- [82] A. Vilenkin, “Unambiguous probabilities in an eternally inflating universe,” *Phys. Rev. Lett.* **81**, 5501-5504 (1998) doi:10.1103/PhysRevLett.81.5501 [arXiv:hep-th/9806185 [hep-th]].
- [83] P. Creminelli, S. Dubovsky, A. Nicolis, L. Senatore and M. Zaldarriaga, “The Phase Transition to Slow-roll Eternal Inflation,” *JHEP* **09**, 036 (2008) doi:10.1088/1126-6708/2008/09/036 [arXiv:0802.1067 [hep-th]].
- [84] B. Freivogel, “Making predictions in the multiverse,” *Class. Quant. Grav.* **28**, 204007 (2011) doi:10.1088/0264-9381/28/20/204007 [arXiv:1105.0244 [hep-th]].
- [85] F. Denef, M. R. Douglas, B. Greene and C. Zukowski, “Computational complexity of the landscape II—Cosmological considerations,” *Annals Phys.* **392**, 93-127 (2018) doi:10.1016/j.aop.2018.03.013 [arXiv:1706.06430 [hep-th]].
- [86] J. Khoury, “Accessibility Measure for Eternal Inflation: Dynamical Criticality and Higgs Metastability,” *JCAP* **06**, 009 (2021) doi:10.1088/1475-7516/2021/06/009 [arXiv:1912.06706 [hep-th]].
- [87] J. Khoury and S. S. C. Wong, “Early-time measure in eternal inflation,” *JCAP* **05**, no.05, 031 (2022) doi:10.1088/1475-7516/2022/05/031 [arXiv:2106.12590 [hep-th]].

# Supplemental Material: Hubble selection of the weak scale from QCD quantum critical point

Sunghoon Jung<sup>1,2,\*</sup> and TaeHun Kim<sup>1,†</sup>

<sup>1</sup>*Center for Theoretical Physics, Department of Physics and Astronomy, Seoul National University, Seoul 08826, Korea*  
<sup>2</sup>*Astronomy Research Center, Seoul National University, Seoul 08826, Korea*

## Appendix A: Quantum critical points of LSM

We present our initial exploration of quantum critical points  $v_h^*$  of the  $N_f = 3$  LSM at tree-level. In Sec. III, we presented the benchmark SM point, Eqs. (6) and (7), that best fits the meson spectrum in Table I. Here we discuss further details of our search and the resulting ranges of best-fit parameters and  $v_h^*$ .

It turns out that  $\lambda_1$  and  $\mu^2$  are least constrained by meson spectrum, as the last three meson observables in Table I have large uncertainties; without such freedom, the tree-level LSM would have been over-constrained. So we vary these two parameters while fixing all others to the benchmark values. We should also focus on the parameter space with  $K > 4.5$  so that coexisting vacua are present at  $\mathcal{H} = 0$ ; this roughly requires  $\mu^2 \lesssim 10$  times the benchmark value.

Fig. 4 shows the numerical results of the critical point  $v_h^*$  (upper panel) and  $\chi^2/\text{dof}$  (lower) as a function of  $\mu^2$  and  $\lambda_1$ ; we denote the values of  $\mu^2$  and  $\lambda_1$  by the ratio (scale factors) relative to the benchmark values, as  $\hat{\mu}^2$  and  $\hat{\lambda}_1$ . We found that  $v_h^*$  is sensitive mostly only to  $\mu^2$ , while  $\chi^2$  only to  $\lambda_1$ . Thus, a wide range of  $v_h^*$  is found to be consistent.

At the  $2\sigma$  confidence level ( $\chi^2/\text{dof} = 4$ ),  $\hat{\lambda}_1 = 0.6 \sim 1.5$  is consistent with all meson observables in Table I, and  $\hat{\lambda}_1 = 0.4 \sim 2.5$  is consistent with first seven observables. Fixing  $\hat{\lambda}_1 = 1$  (or  $\lambda_1 = 7$ ) and restricting  $\hat{\mu}^2 < 10$  (for  $K > 4.5$ ), any values  $v_h^* = \mathcal{O}(1 \sim 100)$  MeV are allowed for some  $\hat{\mu}^2$ . Specifically,  $v_h^* = \Lambda_{\text{QCD}}$  for  $\hat{\mu}^2 \simeq 3$ , and  $v_h^* = 1$  MeV for  $\hat{\mu}^2 \simeq 0.3$ . Although even smaller  $v_h^*$  is allowed with smaller  $\mu^2$ , we do not want too small  $v_h^*$  farther away from  $v_{\text{EW}}$ . In all, as alluded,  $v_h^* = \mathcal{O}(1 - 100)$  MeV can be obtained in the parameter space consistent with meson spectrum, spanned by  $\mathcal{O}(1)$  variations of  $\mu^2$ .

The energy contrast at the critical point does not vary much,  $70 \sim 120$  MeV close to  $\Lambda_{\text{QCD}}$ , in the parameter space shown in the figure.

## Appendix B: Quantum regimes

In Sec. IV, we showed that quantum-dominated evolution falls into two regimes: the global QBC and Q<sup>2</sup>V.

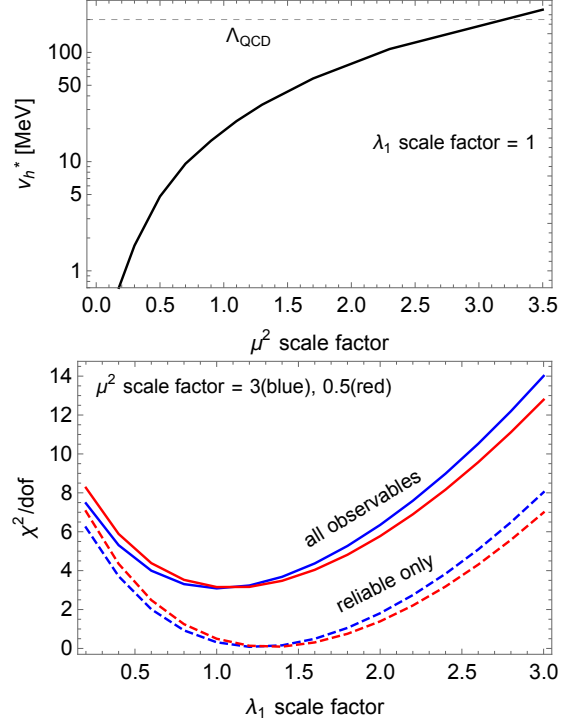


FIG. 4. (Top): Quantum critical point  $v_h^*$  in the  $N_f = 3$  LSM. Other parameters are fixed to benchmark values; scale factors are relative to the benchmark values. (Bottom):  $\chi^2/\text{dof}$  of the global fit to meson spectrum in Table 1.

In this appendix, we discuss further details. We first introduce the QV and Q<sup>2</sup>V regimes derived in [22] and show their equivalence to our results; then we discuss the scaling behaviors of equilibrium solutions, which turn out to provide further intuition as well as useful handles in numerical calculations (see App. C); finally we derive equilibrium properties of Q<sup>2</sup>V near a boundary using the method of images. We also refer to [7, 22, 72] and references therein for other details on FPV solutions.

### 1. Equivalence of quantum regimes

Consider a general class of potential

$$V(\varphi) = V_0 \omega(\varphi), \quad |\varphi| \leq 1 \quad (\text{B1})$$

where the field  $\varphi = \phi/\phi_0$  is normalized by the field range  $\phi_0$ . The potential height is  $V_0 = V(\varphi = 1) - V(\varphi = 0)$  with  $\omega(\varphi = 1) = 1$ ,  $\omega(\varphi = 0) = 0$ , and  $d\omega/d\varphi =$

\* sunghoonj@snu.ac.kr

† gimthcha@snu.ac.kr

$\mathcal{O}(1)$ . Any potential (subdominant to the inflaton's) can be written in this form, by shifting the field and adjusting the potential height by a small constant  $\ll 3M_{\text{Pl}}^2 H_0^2$ .

Up to leading orders of  $V_0 \ll 3M_{\text{Pl}}^2 H_0^2$ , FPV can be written as [22] (assuming  $H_0 \ll M_{\text{Pl}}$ )

$$\frac{\partial \rho(\phi, t)}{\partial T} = \frac{d}{d\varphi} \left( \rho \frac{d\omega}{d\varphi} \right) + \frac{\alpha}{2} \frac{d^2 \rho}{d\varphi^2} + \beta \rho \omega, \quad (\text{B2})$$

where (' denotes the  $\phi$  derivative)

$$\alpha \equiv \frac{3}{4\pi^2} \frac{H_0^4}{V' \phi_0}, \quad \beta \equiv \frac{3\phi_0^2}{2M_{\text{Pl}}^2} \quad (\text{B3})$$

with the dimensionless time  $T \equiv \frac{V'}{3H_0\phi_0} t$  normalized by the characteristic time for classical relaxation  $\sim \phi_0/\dot{\phi} \simeq 3H_0\phi_0/V'$ . In a rough sense,  $\alpha$  comes from the second-derivative diffusion term in FPV, measuring quantum effects;  $\beta$  from the volume term, also measuring the scale of the relevant field range in Planck units. Note that Eq. (B2) depends mostly only on the potential slope, but not on the absolute height as long as it is much smaller than the inflaton potential; this allows to write in the form Eq. (B1). Then [22] argued that the conditions for the QV and Q<sup>2</sup>V regimes are, respectively,

$$\alpha\beta \gtrsim 1, \quad \alpha^2\beta \gtrsim 1. \quad (\text{B4})$$

Applied to our model with  $V_0 = \Lambda_\phi^4$  and  $\phi_0 = f_\phi = M^2/g$  being the full field range, the two conditions read

$$g \lesssim H \frac{H}{M_{\text{Pl}}} \frac{M^2}{\Lambda_\phi^2}, \quad g \lesssim H \frac{H}{M_{\text{Pl}}} \frac{H^2 M^2}{\Lambda_\phi^4}. \quad (\text{B5})$$

These agree with the global QBC in Eq. (11) (not with the local QBC) and the Q<sup>2</sup>V derived in Eq. (13). [22] derived these conditions by requiring the positivity of a dominant eigenmode with absorbing (vanishing) boundary conditions. We rather ended up with the same conditions in yet other ways: the peak climbing up a linear potential, the balance between quantum climbing and boundary repulsion, and the balance width growing larger than Planckian (the minimum allowed by uncertainty principle). It also provided more dynamical explanation of why and how the field range is involved.

Furthermore, since quantum dynamics is set by  $\alpha$  and  $\beta$ , so are equilibrium properties. It was derived in [22] that the width of a localized equilibrium distribution is

$$\sigma_\phi \sim \phi_0 \beta^{-1/2} \simeq M_{\text{Pl}}, \quad \sigma_\phi \sim \phi_0 \left( \frac{\alpha}{\beta} \right)^{1/3}, \quad (\text{B6})$$

for the QV and Q<sup>2</sup>V, respectively. The former always yields the Planckian width (as in our benchmark in Sec. V), the minimum allowed by uncertainty principle; and the latter agrees with our Eq. (12), derived from the local balance near  $\phi_*$ .

## 2. Scaling of equilibrium solution

The key idea in this subsection is that if the equilibrium distribution is well localized, we should be able to get the same solution whether by considering a full field range in FPV or just a large enough range around the distribution. Since the distribution will be localized near the upper boundary (the critical point in this work), solutions must also be largely independent on the lower boundary conditions. Thus, properties of solutions, expressed in terms of  $\alpha$  and  $\beta$ , must scale properly under the re-scaling of the field range considered in FPV.

When it comes to calculate the equilibrium distribution, it is good enough to consider a linear potential, since  $\rho(\phi)$  is localized. Consider a linear potential (in Eq. (B1))

$$\omega(\varphi) = \varphi. \quad (\text{B7})$$

$\varphi = 1$  is the upper boundary or the critical point. The field range  $\phi_0$  does not have to be the full field range, but only needs to contain a large enough range around the critical point.  $\alpha$  and  $\beta$  for this case are

$$\alpha = \frac{3}{4\pi^2} \frac{H^4}{V_0}, \quad \beta = \frac{3}{2} \frac{\phi_0^2}{M_{\text{Pl}}^2}. \quad (\text{B8})$$

Under an arbitrary scaling of the field range by  $a$  (with the upper boundary fixed at the critical point),  $\phi_0 \rightarrow a\phi_0$  and  $V_0 \rightarrow aV_0$ , hence

$$\alpha \propto a^{-1}, \quad \beta \propto a^2. \quad (\text{B9})$$

Thus, the QV and global QBC conditions,  $\alpha\beta \propto a$ , scale proportionally, reflecting again that they encode the necessary field range for Hubble selection. On the other hand, the Q<sup>2</sup>V condition is invariant  $\alpha^2\beta \propto a^0$ , as it measures only the local balance near the upper boundary, as derived in Sec. IV and App. B3.

However, physical properties of equilibrium distributions must remain invariant under such arbitrary scaling. Indeed, the widths in Eq. (B6) are scale invariant as

$$\sigma_\phi \sim \phi_0 \beta^{-1/2} \propto a^0, \quad \sigma_\phi \sim \phi_0 (\alpha/\beta)^{1/3} \propto a^0. \quad (\text{B10})$$

The peak locations (derived in [22] and our App. B3) are also scale invariant as

$$\phi_0 - \phi_{\text{peak}} \sim \frac{\phi_0}{2\alpha\beta} \simeq \frac{4\pi^2}{9} \frac{V' M_{\text{Pl}}^2}{H^4} \propto a^0, \quad \sim \sigma_\phi \propto a^0, \quad (\text{B11})$$

for the QV and Q<sup>2</sup>V, respectively. Notably, the peak location in the QV regime is the same as the minimum field excursion  $\Delta\phi$  needed for a peak to start climbing; this led to the global QBC in Eq. (11).

What do these mean practically? As long as  $\alpha\beta \gtrsim 1$  and  $\sigma_\varphi < 1$ , the same correct solutions can be obtained with any convenient field range around the critical point. If expressed in terms of  $\varphi$ , solutions look broader or narrower just due to different field normalization  $a\phi_0$ . But in terms of physical field value  $\phi$ , they are the same. This can be useful in numerically solving FPV; see App. C.

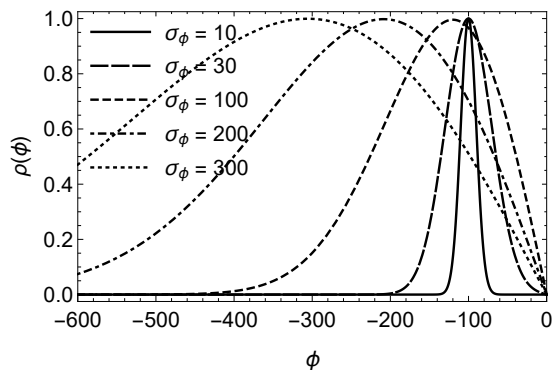


FIG. 5. Effects of the boundary at  $\phi_0 = 0$  on the volume-weighted distribution  $\rho(\phi)$ . For several choices of  $\sigma_\phi$  with fixed  $\Delta\phi = 100$  in the solution Eq. (B12) obtained by the method of images. As the boundary begins to matter (Q<sup>2</sup>V), the distribution becomes pushed away.

### 3. Boundary effects

Lastly, we demonstrate the boundary effects in the Q<sup>2</sup>V regime discussed heuristically in Sec. IV.

In solving FPV, the vanishing boundary condition at  $\phi_0$  is relevant to our work, as any Hubble patches with  $\phi > \phi_0$  (critical point) are out of Hubble selection, hence discarded. The vanishing boundary condition can be imposed by the method of images. Putting two charges at  $\phi_0 \mp \Delta\phi$  and ignoring Hubble expansion for simplicity, we can express the solution in the form [83]

$$\rho(\phi) \propto e^{-\frac{[\phi - (\phi_0 - \Delta\phi)]^2}{2\sigma_\phi^2}} - e^{-\frac{[\phi - (\phi_0 + \Delta\phi)]^2}{2\sigma_\phi^2}}, \quad (\text{B12})$$

where  $\phi < \phi_0$  is the physical region. It describes that, as  $\Delta\phi$  and  $\sigma_\phi$  become comparable, or equivalently as the significant portion of the would-be distribution passes the boundary, the boundary becomes relevant, and the final distribution is displaced away from it. Fig. 5 demonstrates this behavior as a function of  $\sigma_\phi$  for fixed  $\Delta\phi$ . This effectively produces repulsive motion.

But physically, why and how does a boundary affect a peak located away from it? The boundary condition generates the asymmetric absorbing probability, skewing the distribution, which otherwise would be symmetrically quantum diffused. The peak location  $\phi_{\text{peak}}$  is at the extremum satisfying

$$e^{\frac{2(\phi_0 - \phi_{\text{peak}})\Delta\phi}{\sigma_\phi^2}} = \frac{(\phi_0 - \phi_{\text{peak}}) + \Delta\phi}{(\phi_0 - \phi_{\text{peak}}) - \Delta\phi}. \quad (\text{B13})$$

When  $\sigma_\phi \gtrsim \Delta\phi$ , the boundary is most important, and

$$\phi_0 - \phi_{\text{peak}} \simeq \sigma_\phi. \quad (\text{B14})$$

This must be true as  $\sigma_\phi$  is the only dimensionful parameter in this limit. This effectively means repulsive motion

$$\dot{\phi}_b \sim -\frac{d\sigma_\phi}{dt} = -\frac{H^3}{8\pi^2\sigma_\phi}, \quad (\text{B15})$$

justifying the formula for the Q<sup>2</sup>V regime used in Sec. IV.

### Appendix C: Numerical calculation of the equilibrium distribution

In this appendix, we summarize our numerical calculation of the equilibrium distribution  $\rho(\phi)$ . We use the solution given in [22], obtained for a linear potential with the vanishing upper boundary condition, as discussed in App. B2, and here we discuss useful technical steps involved. See also [7, 72] for similar ways to solve FPV at large time.

For the given  $\alpha$  and  $\beta$  in Eq. (B8) from a linear potential Eq. (B7), the equilibrium solution, up to a normalization, is given by [22]

$$\rho(\varphi) \propto e^{-\frac{\varphi}{\alpha}} \left[ \frac{\text{Ai}(x(\varphi))}{\text{Ai}(x(-1))} - \frac{\text{Bi}(x(\varphi))}{\text{Bi}(x(-1))} \right], \quad (\text{C1})$$

where Ai and Bi are the Airy functions with

$$x(\varphi) \equiv a_1 + \left( \frac{2\beta}{\alpha} \right)^{1/3} (1 - \varphi). \quad (\text{C2})$$

$a_1 \simeq -2.3381$  denotes the first zero of Ai. Since the distribution is highly localized, numerical evaluation of  $\rho(\phi)$  often suffers technical difficulties. Close to the upper boundary  $\varphi = 1$ , the solution can be approximated by ignoring small Bi contributions as

$$\rho(\varphi) \propto e^{-\frac{\varphi}{\alpha}} \text{Ai}(x(\varphi)). \quad (\text{C3})$$

For our benchmark Eq. (18) with the upper boundary at the critical point  $\phi_0 = \phi_* = (v_h^*)^2 \lambda_h / g$  and  $V' = \Lambda_\phi^4 / f_\phi = \Lambda_\phi^4 g / M^2$ , we have  $\alpha \simeq 0.05$  and  $\beta \simeq 2 \times 10^4$  so that  $\alpha\beta \simeq 10^3$  (global QBC) and  $\alpha^2\beta \simeq 70$  (Q<sup>2</sup>V marginally). Thus, the width is  $\sigma_\varphi \sim \beta^{-1/2} \sim 0.7\%$  of the field domain  $\phi = [0, \phi_*]$ . This is not so small portion; actually, our benchmark was chosen to ensure this. Therefore, numerical evaluation of  $\rho(\phi)$  in this case does not suffer much technical difficulties. We can convert  $\rho(\phi)$  straightforwardly to  $\rho(v_h)$  using the relation  $v_h^2 = g\phi/\lambda_h$ . In this way, Fig. 3 of the main text is obtained.

More generally, if the width  $\sigma_\varphi$  turns out to be a very small portion of the field domain, then one can use the scaling behavior of App. B2 to reduce the domain and make  $\sigma_\varphi$  larger. In this way, convenient field ranges can be chosen to avoid technical difficulties and readily evaluate Eq. (C3) for equilibrium distributions.